Biochimica et Biophysica Acta 1787 (2009) 68–73

Contents lists available at ScienceDirect

Biochimica et Biophysica Acta

journal homepage: www.elsevier.com/locate/bbabio

The role of the invariant glutamate 95 in the catalytic site of Complex I from *Escherichia coli*

Liliya Euro *, Galina Belevich, Dmitry A. Bloch, Michael I. Verkhovsky, Mårten Wikström, Marina Verkhovskaya *

Helsinki Bioenergetics Group, Institute of Biotechnology, PO Box 65 (Viikinkaari 1) 00014 University of Helsinki, Finland

ARTICLE INFO

Article history:
Received 22 September 2008
Received in revised form 1 November 2008
Accepted 5 November 2008
Available online 13 November 2009

Keywords:
Complex I
NuoF subunit
NADH-binding site

ABSTRACT

Replacement of glutamate 95 for glutamine in the NADH- and FMN-binding NuoF subunit of *E. coli* Complex I decreased NADH oxidation activity 2.5–4.8 times depending on the used electron acceptor. The apparent K_m for NADH was 5.2 and 10.4 μM for the mutant and wild type, respectively. Analysis of the inhibitory effect of NAD^+ on activity showed that the E95Q mutation caused a 2.4-fold decrease of K_i^{NAD+} in comparison to the wild type enzyme. ADP-ribose, which differs from NAD^+ by the absence of the positively charged nicotinamide moiety, is also a competitive inhibitor of NADH binding. The mutation caused a 7.5-fold decrease of $K_i^{ADP\text{-}ribose}$ relative to wild type enzyme. Based on these findings we propose that the negative charge of Glu95 accelerates turnover of Complex I by electrostatic interaction with the negatively charged phosphate groups of the substrate nucleotide during operation, which facilitates release of the product NAD^+. The E95Q mutation was also found to cause a positive shift of the midpoint redox potential of the FMN, from −350 mV to −310 mV, which suggests that the negative charge of Glu95 is also involved in decreasing the midpoint potential of the primary electron acceptor of Complex I.

1. Introduction

The crystallographic structure of the hydrophilic domain of Complex I from *T. thermophilus* shows a cavity close to the cofactor FMN in the catalytic Nqo1 subunit where the NADH may be bound [1,2]. The deep end of this cavity contains two invariant amino acid residues, glutamate 97 and tyrosine 180 that are exposed to the solvent and located in the vicinity of the flavin, and have been suggested to interact with the nicotinamide group of NADH [1]. The double mutation Y204C/C206G in human Complex I (Y204 is the counterpart of Y180 in *T. thermophilus*) causes severe symptoms [3] that could be due to the interaction of these residues with FMN or/and NADH [2]. However, the role of the negatively charged Glu97 has so far not been assessed. Glu97 might cause a decrease of the midpoint redox potential of the non-covalently bound FMN, the value of which was found to be very low (−380 mV [4]; or −350 mV [5]) in comparison to the value of −220 mV for free FMN in aqueous solution. An example of such modulation of the redox properties of non-covalently bound flavin by acidic amino acid residues has been described for flavodoxin from *Clostridium beijerinckii* [6]. Four acidic residues, including Glu97, surround the isoalloxazine ring of the FMN in the *T. thermophilus* Complex I at a distance of 4–6 Å (PDB entry 2FUG, chain 1); each of these residues may contribute to the negative shift of the redox potential of the cofactor. In order to assess the role of the strictly conserved glutamate 97 we mutated the corresponding glutamate 95 in the NuoF subunit of the *E. coli* Complex I to glutamine. Here, we report the consequences of this mutation, which we ascribe to loss of negative charge in the active site.

2. Materials and methods

2.1. 3-D structure prediction of NuoF subunit of E. coli Complex I

Modeling of the NuoF subunit of Complex I from *E. coli* was performed by submitting a model request to a Swiss-Model server [7] (http://swissmodel.expasy.org) using an Alignment Mode. Multiple sequence alignment of 35 homologues of the NuoF subunit from bacterial and eukaryotic genomes sharing not less than 40% of identity was done using ClustalX software (1.81). For homology modeling the sequence of the Nqo1 subunit of *T. thermophilis* Complex I with the known crystal structure (PDB entry 2FUG, chain 1) was chosen as a template. The obtained 3-D model of the NuoF subunit was refined by superposition with the atomic coordinates of the crystal structure of the Nqo1 subunit of *T. thermophilis* Complex I using DeepView/Swiss-PdbViewer software (3.7) [8].

Abbreviations: DDM, n-dodecyl β-D-maltopyranoside; HAR, hexaammineruthenium (III) chloride; DQ, decylubiquinone; dNADH, nicotinamide hypoxanthine dinucleotide reduced sodium salt; ADP-ribose, adenosine 5′-diphosphoribose sodium salt; PMSF, phenylmethanesulfonyl fluoride; FeCy, ferricyanide

* Corresponding authors. Fax: +358 9 191 58003.
E-mail addresses: liliya.euro@helsinki.fi (L. Euro), marina.verkhovskaya@helsinki.fi (M. Verkhovskaya).

0005-2728/$ – see front matter © 2008 Elsevier B.V. All rights reserved.
doi:10.1016/j.bbabio.2008.11.002

2.2. Bacterial strains and site-directed mutagenesis

The used bacterial strains were based on the *E. coli* strain GR70N [9] and the used plasmids are listed in Table 1. Genetic manipulations were carried out using TOP10 (Invitrogen), JM109 and BMH 71-18 *mut*S (Promega) *E. coli* strains. The oligonucleotides used are listed in Table 2.

The NuoF-deficient strain GRF5 was constructed by deleting the internal part of the *nuo*F gene from the chromosomal DNA of the GR70N *E. coli* strain, and replacing it by the unidirectionally transcribing kanamycin resistance cassette.

For this purpose, the *nuo*F gene with up- and downstream regions was amplified from genomic DNA of the *E. coli* GR70N strain with sense UpFF and antisense LowFR oligonucleotides, and the ca. 3 kbp product was ligated in the pGEM-T Easy vector (Promega) resulting in pGEM-LFR. The HincII-fragment of pUC4K containing the Km^R cassette was inserted in the EcoRV and BspEI sites of pGEM-LFR after filling the sticky ends with deoxynucleotide thriphosphates and T4 DNA polymerase yielding pGEM-flF::Km. The NotI-fragment from pGEM-flF::Km containing the kanamycin resistance cassette with flanks complementary to the corresponding regions on chromosomal DNA was ligated into NotI-linearized pKO3. The resulting pKO-flF::Km plasmid was used for the transformation of GR70N competent cells and gene replacement experiments based on homologous recombination as described by Link et al. [10]. The selected kanamycin resistant GRF5 strain had the 998 bp-deletion of the chromosomal *nuo*F gene from 143d to the 1140th oligonucleotide.

The pGEM-LFR vector described above was used as DNA template for mutagenesis. The E95Q point mutation was introduced into pGEM-LFR using the GeneEditor in vitro site-directed mutagenesis system (Promega) according to the manufacturer's instructions, followed by DNA sequencing of the mutated gene. The PspOMI–SalI-fragment of the pGEM-LFR plasmid bearing the point mutation was ligated into NotI–SalI-digested pKO3. The resulting plasmid was used for restoration of the mutated *nuo*F gene on the chromosome of the *nuo*F-deficient GRF5 strain as described by Link et al. [10] with selection of kanamycin-sensitive clones. Correct introduction of the mutation in the chromosome was verified by DNA sequencing.

2.3. Bacterial growth and membrane preparation

Bacteria were routinely grown in LB medium at 37 °C with appropriate antibiotics at indicated concentrations (μg/ml); ampicillin (100); streptomycin (50); kanamycin (50); chloramphenicol (20). Growth tests were carried out under aerobic conditions at 37 °C in rich (LB) and minimal, M9, medium, containing DL-malate as the sole carbon source.

For membrane preparation with further purification of Complex I, the *E. coli* strain GR70N or GRF-E95Q was grown aerobically in a 25 L fermentor in LB medium at 37 °C. The cells were harvested in the late exponential growth phase. Membrane preparation was done as described in [11] with one exception: before passing through an APV Gaulin homogenizer, the cells were suspended in buffer containing 50 mM HEPES/KOH, pH 7.0, 100 mM KCl, 2 mM $MgCl_2$, 0.5 mM PMSF using UltraTurrax.

Table 1
Bacterial strains and plasmids

Strain or plasmid	Genotype/relevant properties	Ref
Strains		
GR70N	F⁻ *thi rps*L *gal*, Sm^R, wild type Complex I	[9]
GRF5	GR70N, *nuo*F::Km^R	This study
GRF-E95Q	GR70N, *nuo*F E95Q	This study
Plasmids		
pGEM-T Easy	Ap^R, PCR product cloning vector	Promega
pUC4K	Ap^R, Km^R, source of kanamycin resistance cassette	Amersham
pKO3	*sac*B, pSC101, Cm^R, gene replacement vector	[10]

Table 2
Oligonucleotides used in this study

Oligonucleotide	Sequence[a]
UpFF	GATCGACTTCGACGTGCGTAAG
LowFR	ACCGAAGTAGACGTTGTCGTGC
FE95Q	CCGATGAAATG***C***AGCCGGGCACC

[a] Mutated nucleotide is in italic bold.

2.4. Purification of Complex I

The purification was based on the protocol described in [11] with the following modifications. For a single purification, membranes with a total of 650–700 mg of protein were used. Membranes were solubilized with DDM (Anatrace) and the extract (140–150 ml) was loaded at a 18 cm/h flow rate onto a 130 ml bed volume of a DEAE–Trisacryl M (BioSepra) column equilibrated with 100 mM NaCl in buffer A containing 50 mM Mes/NaOH, pH 6.0 and 0.05% DDM. Then the column was washed with 400 ml of equilibration buffer and eluted with 200 ml of 180 mM NaCl in buffer A at a 30 cm/h flow rate. Concentrated fractions enriched with Complex I were adjusted to 100 mM of NaCl by dilution with buffer A, then the protein solution was applied onto a 30 ml bed volume of a DEAE–Trisacryl M column at a 17 cm/h flow rate. Then the column was washed with 40 ml of equilibration buffer and eluted at a17 cm/h flow rate with 100 ml of 140 mM NaCl in buffer A.

2.5. Measurements of catalytic activity

HAR and DQ reductase activities of purified or membrane-bound Complex I were measured as described in [11] in the buffer containing 25 mM HEPES–BTP, pH 7.5 and 3.5 mM KCl. FeCy reductase activity was measured in the same buffer in the presence of 50 μM NADH, 1 mM FeCy, and reduction of FeCy was followed at 420 nm (ε=1 mM^{-1} cm^{-1}). For the determination of the inhibitory effect of NAD^+ and ADP-ribose on NADH/HAR oxidoreductase activity of mutated and wild type Complex I, a fixed amount of these chemicals was added into the reaction mixture before the start of the reaction with the protein. Each titration curve presented in this study is the mean of at least three independent measurements.

2.6. Other analytical procedures

Protein concentrations were determined by the BCA protein assay reagent kit (Pierce) with bovine serum albumin as a standard. 10–20% gradient polyacrylamide gels were used for the analysis of purity of wild type and mutated Complex I.

2.7. Optical redox titration

Spectroelectrochemical redox titrations of purified mutated and wild type Complex I were done at pH 7.5 according to the procedure described in [5]. The obtained data were analyzed using MATLAB (The Mathworks, South Natick, MA).

3. Results

3.1. Location of the invariant glutamate 95 in the NADH-binding site of E. coli Complex I

Prediction of the 3-D structure of the NuoF subunit from the *E. coli* Complex I is based on homology modeling using the resolved structure of the *T. thermophilis* Nqo1 subunit as a template (PDB

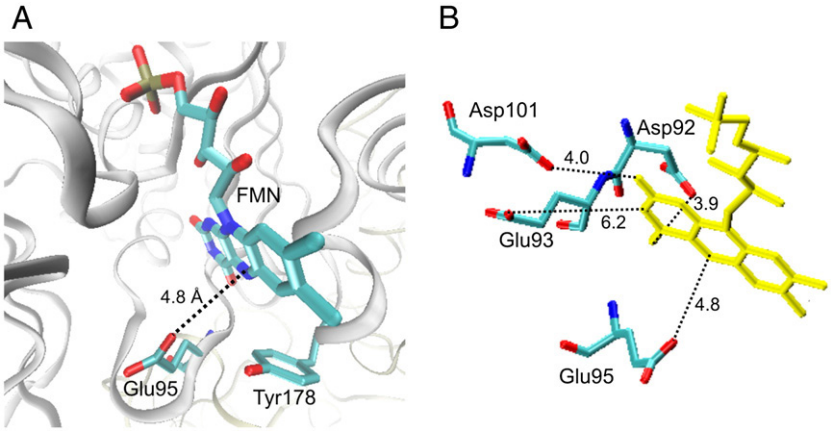

Fig. 1. (A) Location of the invariant E95 and Y178 with respect to the FMN in the NADH-binding site in the modeled NuoF subunit of Complex I from *E. coli*. (B) Conserved negatively charged amino acid residues surrounding the FMN. Atomic distances are represented in Å. Structures are drawn using the VMD program [12].

entry 2FUG, chain 1). E95 in the *E. coli* NuoF subunit, is the counterpart of E97 from Nqo1 in *T. thermophilus* Complex I, and also faces the hydrophilic NADH-binding cavity at a distance of 4.8 Å from the N(3) of the FMN isoalloxazine ring (Fig. 1A). Another three strictly conserved acidic residues (D92, E93 and D101) that surround the flavin have their carboxyl groups located at a distance of 4–6 Å from the isoalloxazine ring of this cofactor (Fig. 1B).

3.2. Activity of membrane bound and purified E95Q mutant of Complex I

Bacterial strains used in this study have two membrane-bound NADH:quinone oxidoreductases: NDH-I (Complex I) and NDH-II (NADH dehydrogenase II), which both oxidize NADH [13]. In order to measure the rate of NADH oxidation by mutated and wild type Complex I in membranes, and to avoid the interference with NDH-II, the analog of NADH, namely dNADH, was used as an electron donor since it is specific only for Complex I. The dNADH:HAR oxidoreductase activity was decreased approximately five times in the E95Q mutant in comparison to wild type, while the rate of dNADH:DQ oxidoreduction declined only 2.5 times. After purification of the wild type and mutated enzymes, their HAR and DQ reductase activities were measured using NADH, and the correlation between the rates of the reactions remained nearly the same as in membranes (Table 3). The rate of NADH oxidation in the purified enzymes was also measured using FeCy, another artificial electron acceptor of Complex I. The NADH:FeCy oxidoreductase activity of the E95Q mutant was decreased 2.5 times relative to wild type, as was the case for the DQ reductase activity.

Analysis by SDS-PAGE (Fig. 2) showed that the decreased rates in the purified E95Q mutant could not be explained by contaminations. The purity of the mutant enzyme was the same as of the wild type.

Table 3
Activities of wild type and mutated Complex I in membrane-bound and purified states

Preparation	Activity, μmol of (d)NADH × min^{-1} × mg^{-1}	
	WT	E95Q
Membranes		
dNADH:HAR reductase	1.9 ± 0.1	0.4 ± 0.1
dNADH:DQ reductase	0.8 ± 0.1	0.3 ± 0.1
Purified Complex I		
NADH:HAR reductase	118.8 ± 7.9	24.4 ± 1.5
NADH:DQ reductase	28.7 ± 2.6	11.5 ± 1.5
NADH:FeCy	127.7 ± 4.5	51.7 ± 2.7

3.3. Kinetic properties of wild type and mutated Complex I

Determination of V_{max} and the apparent Michaelis constants of NADH:HAR oxidoreduction for wild type and mutated Complex I showed that both of these kinetic parameters changed significantly due to the E95Q mutation, which indicates a possible alteration of substrate affinity or/and a disturbance in the catalytic site. The values of V_{max} (138 and 26.5 μmol NADH × min^{-1} × mg^{-1}), K_m^{HAR} (67 and 15 μM) and K_m^{NADH} (10.4 and 5.2 μM) were all decreased significantly in the E95Q mutant, as compared with wild type (Fig. 3). It should be noted that we have determined K_m for HAR for the wild type *E. coli* Complex I as 67 μM, which is much lower than the value of 0.5 mM published in [14] for the bovine enzyme. This difference could be explained by structural differences between the bacterial and mitochondrial enzymes. Since the basic kinetic parameters are only of limited value in a reaction as complicated as that of Complex I, where the mechanism is not known [15], we tested the nucleotide binding site in a more direct way.

Determination of the dissociation constant for NAD^+ can give a clue to the role of glutamate 95 in the NADH-binding site. Competitive inhibition of NADH:HAR reductase activity by NAD^+ in purified wild type Complex I and in the E95Q mutant in the presence of different NADH concentrations is presented as Dixon plots in Fig. 4.

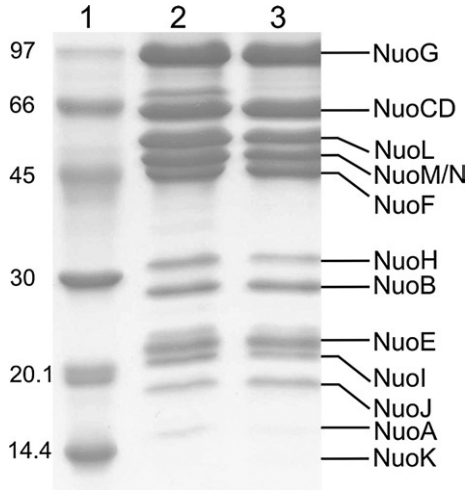

Fig. 2. Coomassie Blue-stained 10–20% SDS-PAGE gel of purified wild type Complex I (lane 2, 30 μg) and E95Q mutant (lane 3, 25 μg). Lane 1: molecular mass markers (kDa). The assignment of the observed bands to individual subunits of Complex I is given on the right.

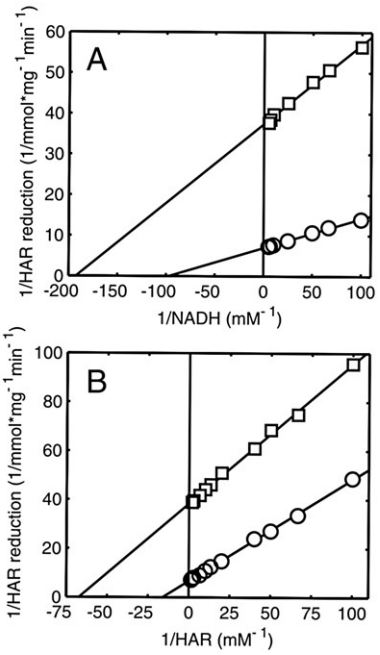

Fig. 3. Double-reciprocal plots for the NADH:HAR reductase reaction catalyzed by purified wild type (circles) and E95Q mutant (squares) Complex I in the presence of 500 μM HAR (A) and 200 μM NADH (B). The activity is expressed as mmol of NADH oxidized by milligram of protein per minute.

NAD^+ is a weak competitive inhibitor. K_i^{NAD+} for the wild type Complex I from *E. coli* was found to be 0.93 mM, and for the mutant this constant decreased approximately 2.4-times to 0.39 mM. This suggests that NAD^+ binds more tightly in the E95Q mutant, dissociating less quickly from the site, thus preventing entrance of a new molecule of NADH.

Since K_i^{NAD+} was determined using NADH:HAR oxidoreductase activity the decreased value of this parameter in the mutant might also be due to an effect of the mutation on HAR binding. To test this possibility we checked the inhibitory effect of NAD^+ on the NADH:DQ oxidoreductase activity of wild type and mutated Complex I in membranes (data not shown). The results of this experiment still clearly showed a similar difference between K_i^{NAD+} for the mutant (0.3 mM) and wild type (1 mM) enzymes, indicating that the mutation affects the NAD-binding site rather than the site where the electron acceptor is bound.

Despite the fact that NAD^+ has a positive charge on the nitrogen atom of the pyridine ring, the total charge of the oxidized nucleotide at neutral pH is negative because of the presence of two phosphate groups. Therefore, the anionic glutamate in the NADH-binding site could be involved in the process of product dissociation by electrostatic repulsion. If this is the case, a change of this amino acid residue to a neutral one should also affect the binding of other negatively charged competitive inhibitors of NADH oxidation, e.g. ADP-ribose [16]. The structure of this compound is similar to NAD^+ but it lacks the positively charged nicotinamide group. To check this suggestion we compared the inhibitory effects of ADP-ribose on NADH:HAR oxidoreductase reaction in purified wild type Complex I and in the E95Q mutant (Fig. 5).

In the wild type enzyme the determined $K_i^{ADP\text{-}ribose}$ (0.97 mM) was comparable to that of K_i^{NAD+}. In contrast, in the mutant the inhibitory effect of ADP-ribose was 7.5 times stronger ($K_i^{ADP\text{-}ribose}$ = 0.13 mM). This finding further supports the notion that the negative charge of Glu95 has the effect of expelling the product NAD^+ from the substrate-binding site.

3.4. Spectroelectrochemical redox titration of the E95Q mutant

Glutamate 95 is one of four conserved negatively charged amino acid residues in the vicinity of FMN (Fig. 1B), which might be involved in maintaining the low redox potential of this cofactor. Consequently, removing one of these negative charges is expected to shift the

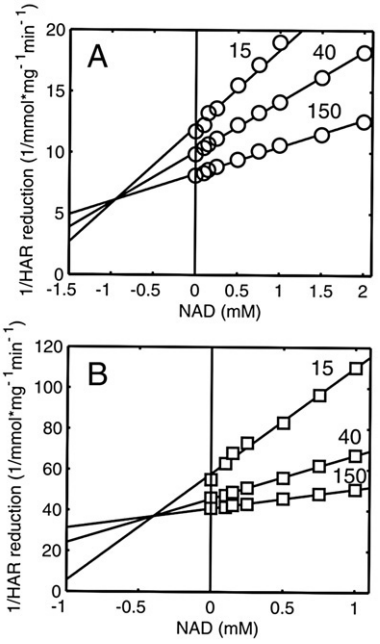

Fig. 4. Competitive inhibition of NADH:HAR reductase activity by NAD+ in purified: (A) wild type (circles) and (B) E95Q mutant (squares) Complex I. Results are presented as Dixon plots; all titrations were done at 350 μM HAR, concentrations of NADH (μM) are indicated above the lines. The activity is expressed as mmol of NADH oxidized by milligram of protein per minute.

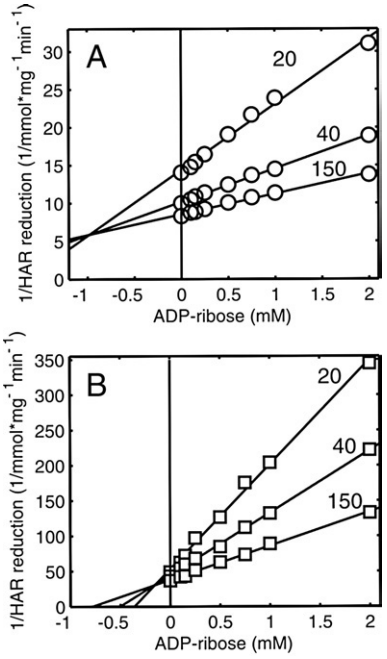

Fig. 5. Competitive inhibition of NADH:HAR reductase activity by ADP-ribose in purified Complex I from wild type (A) and E95Q mutant (B). Results are presented as Dixon plots; all titrations were done at 350 μM of HAR, concentrations of NADH (μM) are indicated above the lines. The activity is expressed as mmol of NADH oxidized by milligram of protein per minute.

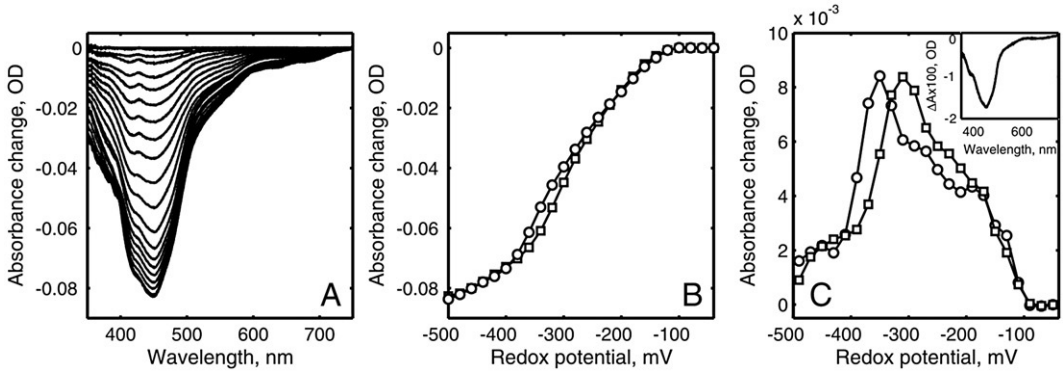

Fig. 6. Optical redox titration of the purified mutated Complex I. (A) Difference spectra (reduced minus oxidized) of the mutant obtained at redox potentials from −500 to −40 mV with step of 20 mV. (B) Titration curves at 450 nm for the wild type (circles) and for the mutant (squares). (C) The first derivatives of the titration curves at 450 nm for the wild type and for the mutant (obtained by subtraction of spectra with adjacent potentials). Inset: the difference spectrum "−320 mV minus −280 mV".

midpoint potential of the flavin to positive values. Electrochemical redox titrations of the purified wild type and E95Q mutant enzymes were carried out using optical spectroscopy. Changes in the spectral region where FMN absorbs maximally are presented in Fig. 6A (optical spectra for wild type Complex I are not shown). Since the oxidized flavin has a very well-defined absorbance maximum at 450 nm, we compared titration curves of the mutant enzyme with the wild type at this wavelength (Fig. 6B). One has to keep in mind that although the iron–sulfur clusters of Complex I are also absorbing in this region, it is nevertheless possible to extract the midpoint redox potential of the two-electron carrier FMN from such data [5]. Comparison of the titration curves of the mutant and wild type enzyme clearly shows that they are nearly the same, except for a component characterized by the maximal slope (Fig. 6B). This component corresponds to the potential range where mostly the FMN spectrum is changing (see inset Fig. 6C). The part of the titration curve with maximal slope was shifted in the mutant relative to the wild type to a more positive redox potential. In order to accurately determine the E_m of the flavin in the E95Q mutant, we plotted the first derivatives of the redox titration curves at 450 nm (Fig. 6C). As seen from this figure, the substitution of glutamate 95 by glutamine caused a positive shift in the midpoint potential of the flavin of 40 mV and resulted in the value of −310 mV (versus −350 mV in wild type [5]). The difference spectrum, −320 mV minus −280 mV (Fig. 6C, inset) from the redox titration of the mutant clearly confirms that the major contribution to the absorbance change in this potential interval indeed derives from a reduced minus oxidized difference spectrum of FMN.

4. Discussion

The analysis of the kinetic parameters of NADH oxidation by wild type and mutated E95Q Complex I indicated that the mutation affects the affinities to both substrate (NADH) and product (NAD^+) of the reaction and decreases the turnover of the enzyme. A drop by a factor of 2.5 in the rate of NADH oxidation by the mutant Complex I was observed if FeCy or ubiquinone were used as an electron acceptors, but in the case of HAR the V_{max} appeared to be 5 times less than in the wild type. This suggests that in the first two cases the glutamate replacement altered either nucleotide binding/debinding or/and the efficiency of the electron transfer from NADH to FMN, while in the latter case the mutation may additionally cause a change in the affinity for HAR which would be in line with an idea suggested by Zickermann et al. [17].

Since Glu95 has its side chain oriented towards the NADH-binding cavity located in front of the FMN at a distance of 4.8 Å from N(3) of its isoalloxazine ring (Fig. 1A), the suggestion that E95 interacts with the nicotinamide moiety of NADH [1] looks solid. Therefore, replacement of the acidic Glu by the neutral Gln is *a priori* expected to lead to a decrease in the affinity for NAD^+, because of loss of electrostatic attraction between the negatively charged carboxyl group of Glu95 and the positively charged nitrogen of the pyridine ring. However, the opposite effect was observed. Here, one should take into account that the *overall* charge of the NAD^+ molecule is negative because of the two phosphate groups, making electrostatic *repulsion* between the Glu95 anion and the nucleotide a definite possibility. We therefore suggest that the main role of E95 is not in the binding of NADH, but rather in promoting the dissociation of the product NAD^+ due to electrostatic repulsion. This is in line with the finding that the affinity of the mutated Complex I for ADP-ribose, which lacks the positive nicotinamide moiety, was increased even further than that in case of NAD^+.

Based on the resolved crystal structure of the hydrophilic domain of *T. termophilus* Complex I it was suggested that the residues 66–69 from the glycine-rich loop of Nqo1 are involved in binding of the nucleotide phosphate groups [1]. Our proposal does not contradict this conclusion since the distances from Glu97 to Gly66 and Gly67 (5.5 Å and 7.4 Å, respectively), are short enough for electrostatic interactions between glutamate 97 and the phosphate groups if the residues from the glycine-rich loop indeed participate in coordination of the latter. Almost the same distances between E95 and the corresponding glycines 63 and 64 (5.4 Å and 7.4 Å, respectively) can be predicted from the modeled structure of the NuoF subunit from *E. coli*.

The hydride transfer from NADH to FMN, the planar condensed rings systems of which are likely positioned in parallel and close to each other in the cavity [1], is expected to be very fast. Likewise, further electron transfer via the iron–sulfur centers is also fast [18]. Hence, the overall rate of the reaction should be determined either by the rate of substrate binding (NADH or HAR^{ox}) or product release (NAD^+ or HAR^{red}). Since the rate of NADH oxidation also decreased by the mutation when ferricyanide or ubiquinone were used as electron acceptors, the effect of the mutation is likely to be determined by a change in the affinity to nucleotides. We have previously reported that the rate of NADH binding is very fast, whereas dissociation of the product NAD^+ is much slower and likely to be rate-limiting [18]. Our current data is in accordance with this proposal. A higher affinity for NAD^+ should decrease the activity of the enzyme, as observed with the E95Q mutant. Therefore, the negative charge of the glutamate in the substrate-binding site located close enough to the phosphates of the nucleotide might have the purpose of fine-tuning the site to effectively expel product.

Another evident role of the negatively charged glutamate in the vicinity of FMN is to decrease the redox potential of the latter. Since free flavin has an E_m of −220 mV and the E_m of the NADH/NAD^+ pair is −320 mV, the downshift of the midpoint potential of the protein-bound FMN is probably important for an enzyme such as Complex I

that functions under conditions close to equilibrium. The E_m value of FMN in Complex I is −350 mV [5]. Our current results demonstrate that Glu95, as one of the four negatively charged amino acid residues surrounding the flavin, has a share of 40 mV of the overall 130 mV depression of the midpoint potential of the primary electron acceptor in Complex I.

Acknowledgements

This work was supported by Biocentrum Helsinki, the Sigrid Jusélius Foundation, the Academy of Finland and Helsinki Graduate School in Biotechnology and Molecular Biology (to L.E.). We thank Eija Haasanen for an excellent technical assistance.

References

[1] L.A. Sazanov, P. Hinchliffe, Structure of the hydrophilic domain of respiratory complex I from *Thermus thermophilus*, Science 311 (2006) 1430–1436.
[2] L.A. Sazanov, Respiratory complex I: mechanistic and structural insights provided by the crystal structure of the hydrophilic domain, Biochemistry 46 (2007) 2275–2288.
[3] P. Benit, D. Chretien, N. Kadhom, P. Lonlay-Debeney, V. Cormier-Daire, A. Cabral, S. Peudenier, P. Rustin, A. Munnich, A. Rotig, Large-scale deletion and point mutations of the nuclear NDUFV1 and NDUFS1 genes in mitochondrial complex I deficiency, Am. J. Hum. Genet. 68 (2001) 1344–1352.
[4] V.D. Sled, N.I. Rudnitzky, Y. Hatefi, T. Ohnishi, Thermodynamic analysis of flavin in mitochondrial NADH:ubiquinone oxidoreductase (complex I), Biochemistry 33 (1994) 10069–10075.
[5] L. Euro, D.A. Bloch, M. Wikstrom, M.I. Verkhovsky, M. Verkhovskaya, Electrostatic interactions between FeS clusters in NADHubiquinone oxidoreductase (complex I) from *Escherichia coli*, Biochemistry 47 (2008) 3185–3193.
[6] L.H. Bradley, R.P. Swenson, Role of glutamate-59 hydrogen bonded to N(3)H of the flavin mononucleotide cofactor in the modulation of the redox potentials of the *Clostridium beijerinckii* flavodoxin. Glutamate-59 is not responsible for the pH dependency but contributes to the stabilization of the flavin semiquinone, Biochemistry 38 (1999) 12377–12386.
[7] T. Schwede, J. Kopp, N. Guex, M.C. Peitsch, SWISS-MODEL: an automated protein homology-modeling server, Nucleic Acids Res. 31 (2003) 3381–3385.
[8] N. Guex, M.C. Peitsch, SWISS-MODEL and the Swiss-PdbViewer: an environment for comparative protein modeling, Electrophoresis 18 (1997) 2714–2723.
[9] G.N. Green, R.G. Kranz, R.M. Lorence, R.B. Gennis, Identification of subunit-I as the cytochrome-B558 component of the cytochrome-D terminal oxidase complex of *Escherichia coli*, J. Biol. Chem. 259 (1984) 7994–7997.
[10] A.J. Link, D. Phillips, G.M. Church, Methods for generating precise deletions and insertions in the genome of wild-type *Escherichia coli*: application to open reading frame characterization, J. Bacteriol. 179 (1997) 6228–6237.
[11] G. Belevich, L. Euro, M. Wikström, M. Verkhovskaya, Role of the conserved arginine 274 and histidine 224 and 228 residues in the NuoCD subunit of complex I from *Escherichia coli*, Biochemistry 46 (2007) 526–533.
[12] W. Humphrey, A. Dalke, K. Schulten, VMD: visual molecular dynamics, J. Mol. Graph. 14 (1996) 33–38.
[13] K. Matsushita, T. Ohnishi, H.R. Kaback, NADH-ubiquinone oxidoreductases of the *Escherichia coli* aerobic respiratory chain, Biochemistry 26 (1987) 7732–7737.
[14] E.V. Gavrikova, V.G. Grivennikova, V.D. Sled, T. Ohnishi, A.D. Vinogradov, Kinetics of the mitochondrial three-subunit NADH dehydrogenase interaction with hexammineruthenium(III), Biochim. Biophys. Acta 1230 (1995) 23–30.
[15] A.D. Vinogradov, NADH/NAD+ interaction with NADH: Ubiquinone oxidoreductase (complex I), Biochim. Biophys. Acta 1777 (2008) 729–734.
[16] T.V. Zharova, A.D. Vinogradov, A competitive inhibition of the mitochondrial NADH-ubiquinone oxidoreductase (Complex I) by ADP-ribose, Biochim. Biophys. Acta 1320 (1997) 256–264.
[17] V. Zickermann, S. Kurki, M. Kervinen, I. Hassinen, M. Finel, The NADH oxidation domain of Complex I: do bacterial and mitochondrial enzymes catalyze ferricyanide reduction similarly? Biochim. Biophys. Acta 1459 (2000) 61–68.
[18] M.L. Verkhovskaya, N. Belevich, L. Euro, M. Wikstrom, M.I. Verkhovsky, Real-time electron transfer in respiratory complex I, Proc. Natl. Acad. Sci. U. S. A. 105 (2008) 3763–3767.